CIRP Seminar on Micro and Nano Technology
Copenhagen, Denmark, November 13-14, 2003

# Energy Harvesting MEMS Devices Based on $d_{33}$ Mode Piezoelectric $Pb(Zr,Ti)O_3$ Thin Film Cantilever

Yongbae Jeon, Rajendra Sood, Lodewyk Steyn, and Sang-Gook Kim
Micro and Nano Systems Laboratory, Dept. of Mechanical Engineering
Massachusetts Institute of Technology
Cambridge, MA 02139, USA

**Abstract**

A thin film lead zirconate titanate, $Pb(Zr,Ti)O_3$ (PZT), MEMS-based cantilever device is developed. It uses the $d_{33}$ piezoelectric mode and is fabricated with only three mask steps. The 170μm long piezoelectric cantilever device, called the Piezoelectric Micro Power Generator (PMPG), was designed to harvest ambient vibrational energy. It has a mechanical resonance frequency of 13.7kHz and has shown that it can deliver 1 μW of continuous electrical power to a resistive load at 2.3V DC. The maximum closed-circuit charge amplitude is 13.2 pC at 13.7 kHz, which corresponds to a maximum cantilever tip displacement of 2.56 μm during base shaking experiments. A 3V DC voltage across the resistive load is also a big benefit of the $d_{33}$ type piezoelectric device we developed. This piezoelectric micro cantilever device could be used for various applications such as batteryless micro sensors and micro power generators.

**Keyword**:
piezoelectric, MEMS, thin film

## 1. INTRODUCTION

Energy harvesting is an area of active research. Many methods have been employed for harvesting energy from the environment. The most familiar ambient energy source is solar power. Other examples include electromagnetic fields (used in RF powered ID tags, inductively powered smart cards, etc.), thermal gradients, fluid flow, energy produced by the human body, and the action of gravitational fields. Finally, vibrational energy can be used as an ambient source. A power generator based on transducing mechanical vibrations can be enclosed to protect it from a harsh environment, and it functions in a constant temperature field.

The most immediate applications for such a device is to power micro sensors and/or low power very large scale integration (VLSI) circuits. Aggressive power scaling trends over the last decade have resulted in power consumption in only the 10's to 100's of μW for low to medium throughput Digital Signal Processing (DSP) circuits and other digital VLSI circuits. As these power trends improve, energy harvesting devices become more viable as portable power sources over ordinary chemical batteries. Digital VLSI technology requires an "on" voltage of approximately 3V or more. In order to accomplish such a high voltage, the piezoelectric energy harvesting method is most useful, especially with the $d_{33}$ piezoelectric mode. The Piezoelectric Micro Power Generator (PMPG) is a MEMS based device designed to harvest vibrational energy from the ambient source. It can generate a high open circuit voltage suitable for voltage rectification and for powering low power VLSI circuits. We envision that several PMPG devices could generate power on the order of 10 μW within an area of approximately 1 $mm^2$.

PZT thin films have attracted attention for many applications such as accelerometers [1], force sensors [2], actuators [3], gyroscopes [4], micro pumps [5], tunable optics [6, 7], ferroelectric RAM [8], and display systems [9]. PZT MEMS devices have many advantages such as fine resolution, large force generation, fast response time, zero magnetic fields, low power consumption, vacuum and clean room compatibility and operation at cryogenic temperatures. However, it is more difficult to fabricate a PZT MEMS device versus a similar beam-structured electrostatic device because PZT film is not a normal material for general silicon processing, often requiring many more mask steps.

Piezoelectric $d_{31}$ type sensors and actuators have a cantilever beam structure that consists of a membrane film, bottom electrode, piezoelectric film, and top electrode. The $d_{31}$ type devices require many mask steps (3~5 masks) for patterning of each layer while have very low induced voltage. A generated open circuit voltage (V) can be induced between the electrodes through an applied, external stress ($\sigma_{xx}$) and is expressed in equation (1):

$$V = \sigma_{xx} g_{31} t_{pzt} \qquad (1)$$

where $g_{31}$ (unit is V·m/N) is the transverse piezoelectric coefficient and $t_{pzt}$ is the thickness of the PZT thin film. Piezoelectric cantilevers which use an interdigitated (IDT) top electrode to employ the $d_{33}$ type piezoelectric mode do not have a bottom electrode and can generate electrical power with quit high induced voltage. Its structure is shown in Figure 1(a). The figure 1(b) is a cross-sectional view. It shows the alternating plus and minus potentials that are imposed on the adjacent mini-electrodes (which together make up the interdigitated electrode) when the PZT is poled. The right side of the diagram is a top view of the interdigitated electrode.

A generated open circuit voltage (V) can be induced by external stress ($\sigma_{xx}$) due to the longitudinal, piezoelectric coefficient as demonstrated in equation (2):

$$V = \sigma_{xx} g_{33} L \qquad (2)$$

where L is the distance between the IDT electrodes. Because the magnitude of the $g_{33}$ is 2 to 2.5 times larger than its $g_{31}$ counterpart, and since L can be much bigger than $t_{pzt}$ , the open-circuit voltage of $d_{33}$ type sensors is expected to be much larger (20 times or greater) than $d_{31}$ type sensors of similar dimensions (See Figure 2).
This paper investigates a $d_{33}$ type piezoelectric microcantilever that has increased sensitivity and a streamlined fabrication process with a reduced number of

photo steps. The cantilever structure is released by an isotropic $XeF_2$ vapor etch step, which avoids stiction.

## 2. DESIGN AND FABRICATION

### 2.1 Design

Figure 1 shows the device schematic of the $d_{33}$ mode piezoelectric device. The basic design of the multilayer structure is as follows: Layer 1: Membrane layer ($SiO_2$) for controlling stress and bow of the cantilever structure; Layer 2: Diffusion barrier/buffer layer ($ZrO_2$) for preventing electrical charge diffusion from the piezoelectric layer above it; Layer 3: PZT piezoelectric layer; Layer 4: Top interdigitated electrode (Pt/Ti). Layer 5: Optional SU-8 Proof Mass.

The mechanical resonance frequency of the cantilever can be tuned by altering the cantilever dimensions (i.e. layer thicknesses, length of the beam and the inclusion of a proof mass, if necessary). This affects the k stiffness of the composite beam. The resonance frequency can be approximated by calculating the composite beam stiffnes, K, the value of the lumped mass, M (A proof mass was included in our experimental device.) and using the standard formula for the resonance frequency, $\omega_n$:

$$\omega_n = \sqrt{\frac{K}{M}} \tag{3}$$

The vibrational excitation of the PMPG micro cantilever can be modeled as a seismically excited, spring-mass damper:

$$M\ddot{x}_o + B\dot{x}_o + Kx_o = Kx_i + B\dot{x}_i \tag{4}$$

where $x_i$ is the input, seismic base displacement, $x_o$ is the output, cantilever tip displacement, M is the lumped mass, B is the damping coefficient and K is the stiffness of the composite cantilever beam.

The ratio of the cantilever tip displacement to base displacement at resonance is a well known result as shown in equation (5):

$$\left| \left. \frac{x_o(s)}{x_i(s)} \right|_{s=j\omega_n} \right| = \left| \left. \frac{w_n^2 + 2\xi w_n \cdot s}{s^2 + 2\xi w_n \cdot s + w_n^2} \right|_{s=jw_n} \right| = Q$$

$$\text{where} \quad \xi = \frac{1}{2Q} \quad \text{and} \quad Q = \frac{M\omega_n}{B} \tag{5}$$

The Q of the system can be found by taking the ratio of the tip displacement at resonance over the tip displacement far outside the resonance. For the actuation mode the Q turns out to be approximately 47. It is expected to be higher for the sensor mode.

The rectification bridge circuit consists of four STMicroelectronics® 1N5711 small signal Schottky diodes and a 10 nF mylar storage capacitor. These diodes were chosen specifically because, compared to most discreet components, they have the smallest forward voltage drop (approximately 0.2V). This allows for the largest possible DC voltage to develop across the cap/load. The 10 nF mylar cap was chosen because it does not leak currently easily. The resistors are also discreet components.

### 2.2 Fabrication

We fabricated a $d_{33}$ mode, thin film PZT cantilever device with IDT electrode using just three photo masks. First, the membrane layer (PECVD oxide) is deposited on the Si wafer. Each PECVD oxide layer is annealed at 750°C for 30 minutes. The 50 nm thick $ZrO_2$ layer is deposited via a sol-gel spin-on process. It acts as a buffer layer on top of the various membrane layers and is dried at 350°C for 1 minute, then annealed at 700°C for 15 minutes. Our device uses 0.05μm $ZrO_2$/0.4μm PECVD oxide.

The PZT solution is spun on the substrate at 500 rpm for 3 seconds and 1500 rpm for 30 seconds. The precursor gel film is pyrolyzed at 350°C for 5 minutes on a hot plate in several repeated cycles to create a PZT layer with 0.48 um thickness. The PZT film is annealed at 700°C for 15 minutes in a box furnace. The PZT layer and membrane layers are patterned via RIE with the first mask. The interdigitated top electrode requires the second mask and is deposited using an e-beam evaporation and lift-off procedure with 20nm Ti and 200nm Pt. The SU-8 is spin coated on top of the existing layers and patterned with the third mask to create the proof mass. The cantilever membrane is then released with the $XeF_2$ vapor etcher. No mask is required because $XeF_2$ has a high etch selectivity between Si and the other layers. An SEM image of the fabricated PMPG device is shown in Figure 3.

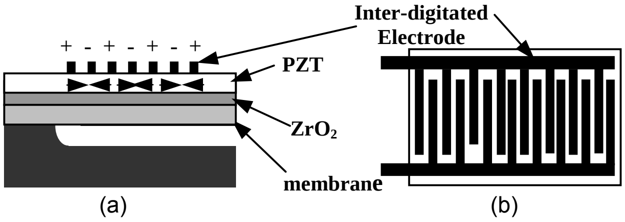

(a) (b)

Figure 1: Device schematic of $d_{33}$ mode piezoelectric device.

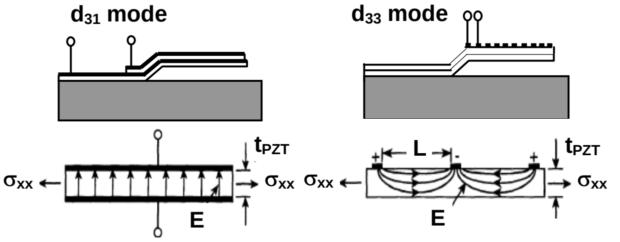

$V_{31} = \sigma_{xx} \bullet t_{pzt} \bullet g_{31}$ $V_{33} = \sigma_{xx} \bullet L \bullet g_{33}$

$V_{33} = 2L / t_{pzt} \bullet V_{31} \cong 20 \bullet V_{31} \cong 3\ V$

( if $g_{33} > 2g_{31}$, $L \cong 10\ t_{PZT}$)

Figure 2: Higher $d_{33}$ Open Circuit Voltage vs. $d_{31}$

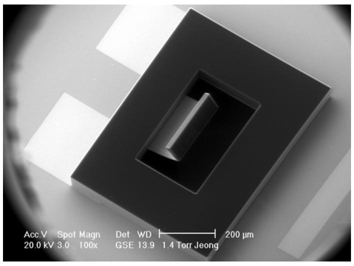

Figure 3. SEM image of the fabricated device

### 2.3 Packaging, Poling and Assembly

The MEMS chip with multiple PMPG devices was super glued to a multiple pin, ceramic package. Each MEMS device has two bond pads: One for the positive potential and one for the negative. The chip was packaged using wire bonding. Two package pins are required for each MEMS device (plus and minus). Finally, electrical wire was stripped and soldered directly to the exposed pins on the back of the package in order to interface with the measurement electronics (charge amplifier) and proto board containing the external rectification circuitry and resistive load. The packaging was covered with a glass lid to prevent environmental contamination.

After packaging, the devices were poled using a hot plate and high voltage DC power supply. The packaged MEMS chip was heated to 100 °C and poled at 90V DC for 30 minutes. The temperature was then cooled down to room temperature while maintaining the 90 V applied voltage. Once the chip is at room temperature, the applied field can be removed.

Post assembly involved creating the rectification circuitry on a protoboard. The load resistance was varied and placed in parallel with the storage cap. A simple, RC high pass filter circuit was also placed on the protoboard and used to remove low frequency (60 Hz) electrical noise from the generated electrical signal before being measured with the oscilloscope.

## 3. EXPERIMENTAL RESULTS AND DISCUSSION

### 3.1 PMPG Direct Excitation

The first set of experiments involved operating the device in the actuation mode (applying an AC voltage signal directly to the device in order to actuate it). The device was excited with a ±3V AC drive voltage from 0 to 200 kHz in order to determine the first mode resonance frequency. Figure 4 shows the first, second and third mode resonance peaks of the PMPG device during direct excitation. First mode resonance was determined to be approximately 13.9 kHz. The resonance peak shifts down a little to 13.7 kHz in the sensor mode (base shaking experiments). In a separate experiment, our 170 μm long cantilever device achieved a tip displacement of 4.66μm under a ±5V driving voltage in first mode resonance. A laser vibrometer system was used to detect the cantilever tip displacement.

### 3.2 Base Shaking Experiments

Base displacement is simply the displacement of the silicon substrate to which the micro cantilever is attached. In order to prove the piezoelectric energy harvesting concept, the PMPG device was shaken by a piezoelectric shaker at the first mode resonance frequency of 13.7 kHz. During these base shaking experiments, the magnitude of the base displacement was varied by varying the shaker drive voltage. Figure 5 shows the base displacement magnitude versus resulting cantilever tip displacement magnitude. Increasing the cantilever tip displacement causes increased amounts of charge to develop on the IDT electrode structure. This is due to the increased axial stress developed within the PZT thin film layer. The generated, closed-circuit charge was measured with a charge amplifier. The maximum generated charge was measured at 13.2 pC peak amplitude. These results are shown in Figure 6.

For the next set of base shaking experiments, the PMPG device was connected to a bridge rectifying circuit with a resistive load across the storage capacitor. The base displacement magnitude was fixed, as was the shaking frequency at 13.7 kHz. The electrical equivalent model of the total PMPG power system (MEMS device + power rectification circuit and resistive load) is shown in Figure 7.

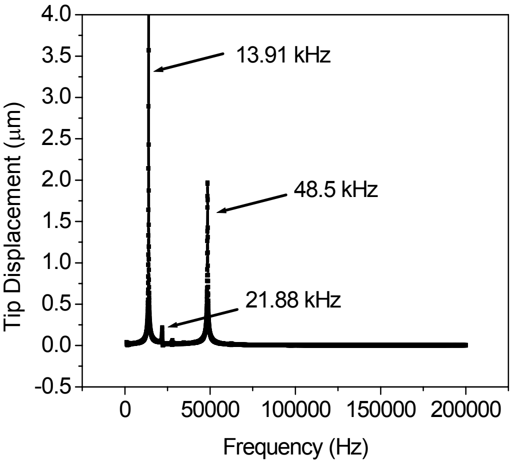

Figure 4: Frequency Response of Cantilever Tip Displacement Due to Direct Excitation. First mode resonance frequency of the excitation mode is approximately 13.9 kHz.

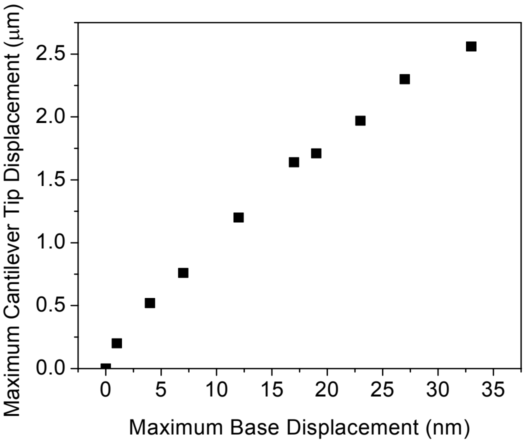

Figure 5: Cantilver Tip Displacement During Base Shaking at Resonance (13.7kHz)

Figures 8 and 9 show the load voltage and power delivered to the load as a function of the load resistance at 13.7 kHz resonance. As expected, the load voltage increases with the increased load. However, the power delivered to the load will not increase indefinitely. There is a maximum point, after which the transferred electrical power will decrease as a result of increased load resistance. In our experiments this occurred when the 10.1 MΩ resistance was inserted into the power system. Some specific load resistance in-between the 5.2 MΩ and 10.1 MΩ loads would define the exact maximum point. Maximum base displacement was measured at 14 nm during base shaking. Generated, closed-circuit charge was measured at 12.2 pC amplitude prior to electrical loading.

The highest DC voltage of 3V was achieved with the 10.1MΩ load. The highest transferred power of 1.01 μW occurred for the 5.2 MΩ load. The storage capacitor charging and discharging times were approximately 0.2 and 0.3 seconds, respectively.

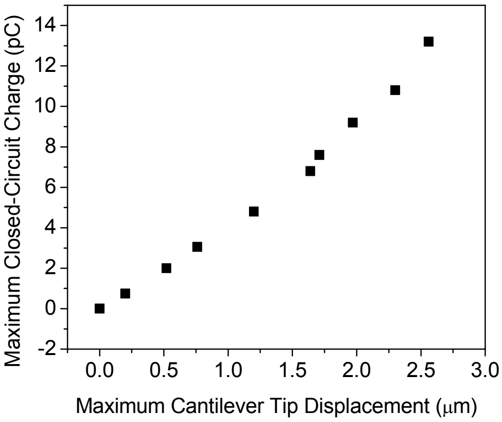

Figure 6: Generated Closed-Circuit Charge Amplitude from Cantilever Tip Displacement

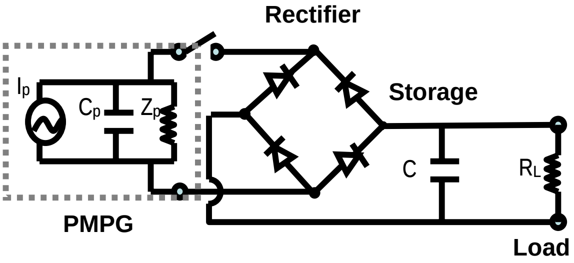

Figure 7: Equivalent Electrical Model of PMPG Power System

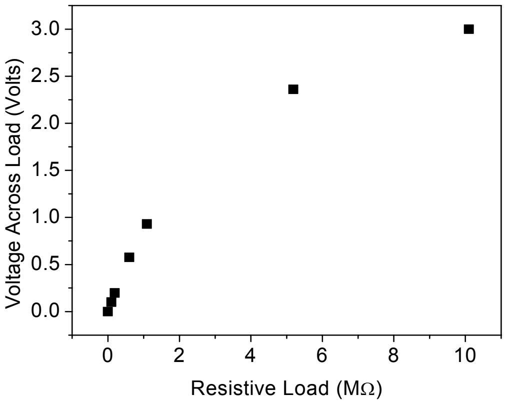

Figure 8: Voltage Across Load Resistor vs. Load Resistance at 13.7 kHz Resonance

## 4. SUMMARY

We have designed, fabricated, and demonstrated a $d_{33}$ type PZT thin film cantilever device using three photo masks. The device has a 1st mode resonance frequency of 13.7 kHz. A 5V amplitude drive signal at resonance resulted in a 4.66 μm tip displacement during actuation mode. The maximum, generated, closed-circuit charge amplitude was measured at 13.2 pC for a tip displacement of 2.56 μm in the sensor mode. A maximum DC voltage of 3V was induced across the load (10.1 MΩ), and a continuous electrical power of over 1μW was delivered to the 5.2 MΩ load. It has been show that the $d_{33}$ mode thin film piezoelectric cantilever device could be used for micro actuators, sensors and piezoelectric micro power generation by scayenging ambient vibrational energy as an energy source.

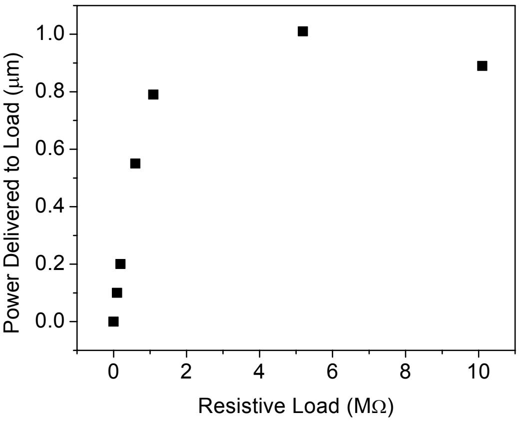

Figure 9. Power Delivered to Load Resistor vs. Load Resistance at 13.7 kHz Resonance

## 5. REFERENCES

[1] Y. Nemirovsk, A. Nemirovsky, P. Muralt, and N. Setter, “Design of a novel thin-film piezoelectric accelerometer”, Sensors and Actuators A 56 (1996), 239-249

[2] C. Lee, T. Itoh, and T. Suga, “Micromachined piezoelectric force sensors and based on PZT thin films”, IEEE Transaction on Ultrasonics, Ferroelectrics, and Frequency control, vol.43, No.4, July (1996), 553-559

[3] P. Schiller and D.L. Polla, “Integrated piezoelectric microactuators based on PZT thin films”, The 7th International Conference on Solid-State Sensors and Actuators, (1994 ), 154-157

[4] T. Fukuda, H. Sato, F. Arai, H. Iwata and K. Itoigawa, “Parallel Beam micro sensor/actuator unit using PZT thin films and its application examples”, Proceedings of the 1998 IEEE Internaitonal Conference on Rootics & Automation, Belgium, May (1998), 1498

[5] Richard M. White, “Silicon based Ultrasonic microsensors and micropumps”, Integrated Ferroelectrics, Vol. 7 (1995), 353-358

[6] S.G. Kim, C. Wong and Y. Jeon, “Strain-tuning of Optical devices with Nanometer Resolution”, Annals of the CIRP, Vol. 52, 2003

[7] C.W. Wong, Y.B. Jeon, G. Barbastathis, S.-G. Kim, “Analog Tunable Gratings Driven Via Thin-Film Piezoelectric MEMS Actuators”, Applied Optics, Vol 42, No. 4, (2003), pp 621-626

[8] J.F. Scott and C.A. Araujo, Science 246, (1989), 1400

[9] S.G. Kim, K.H. Hwang, J. Hwang, M.K. Koo, and K.W, Lee, "Thin-film Micromirror Array (TMA) - A New Chip-based Display Device for the Large Screen Display", *Journal of the Society of Information Display,* Vo. 8, No. 2, (2000)